Nguyen et al., https://doi.org/10.1083/jcb.201607039

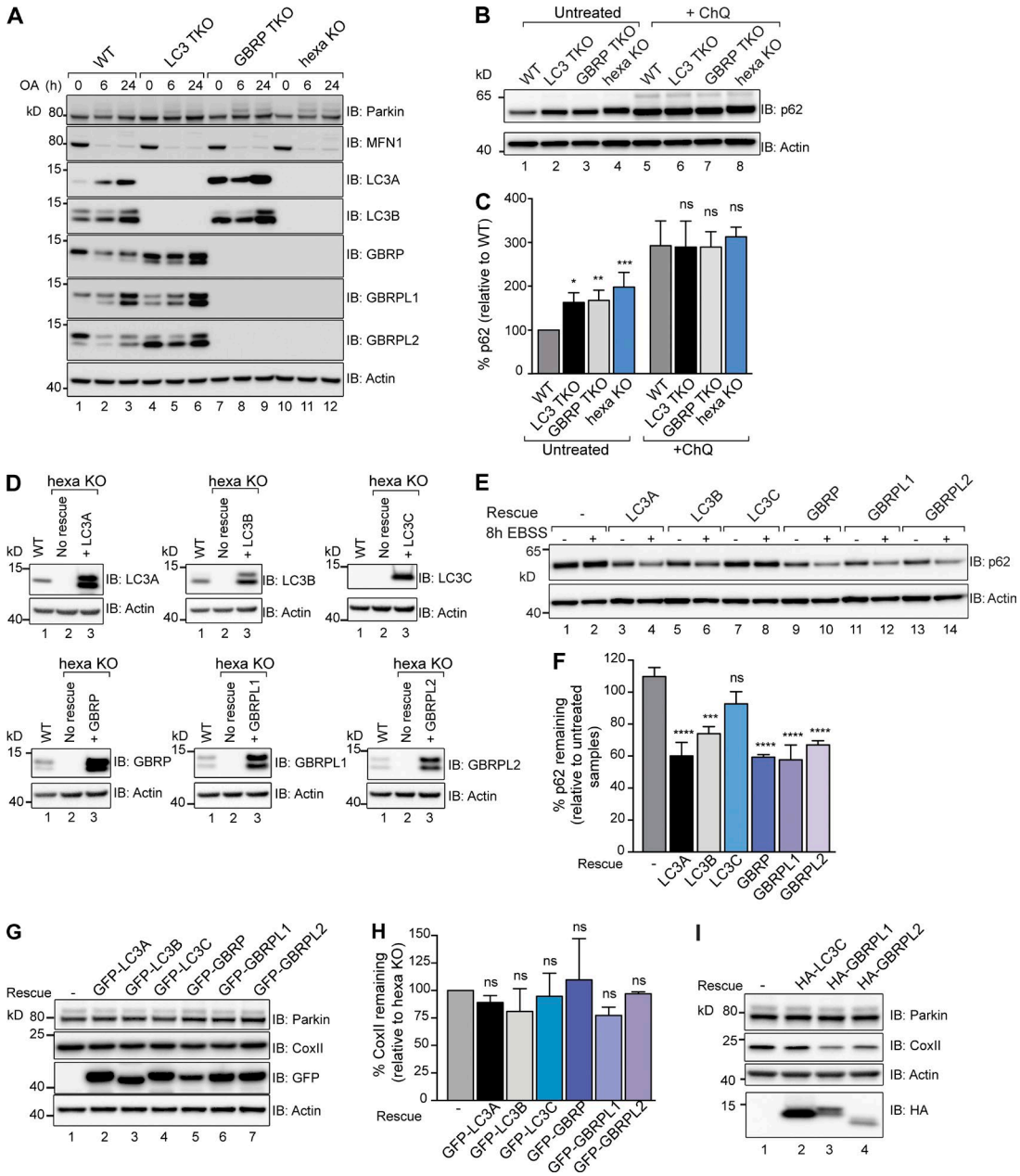

Figure S1. **Analysis of KO and rescue cell lines.** (A) Expression profile of LC3s and GBRPs in WT, LC3 TKO, GBRP TKO, and hexa KO expressing mCh-Parkin upon a mitophagy induction time course IB, immunoblot. (B and C) p62 levels in untreated and chloroquine (ChQ)–treated WT, LC3 TKO, GBRP TKO, and hexa KO were analyzed by immunoblotting (B) and quantified (C). (D) Expression levels of untagged LC3s/GBRPs in hexa KO rescue lines. (E and F) hexa KO rescued with individual untagged LC3s or GBRPs fully fed or starved with EBSS were analyzed by immunoblotting (E), and p62 levels were quantified (F). (G and H) Lysates from hexa KO cells expressing GFP-tagged Atg8 proteins were immunoblotted (G), and CoxII levels were quantified (H). (I) Hexa KO cells expressing mCh-Parkin and HA-tagged LC3C, GBRPL1, or GBRPL2 were analyzed by immunoblotting. Data in C, F, and H are mean ± SD from three independent experiments. *, P < 0.05; **, P < 0.005; ***, P < 0.001; ****, P < 0.0001 (one-way ANOVA). ns, not significant.

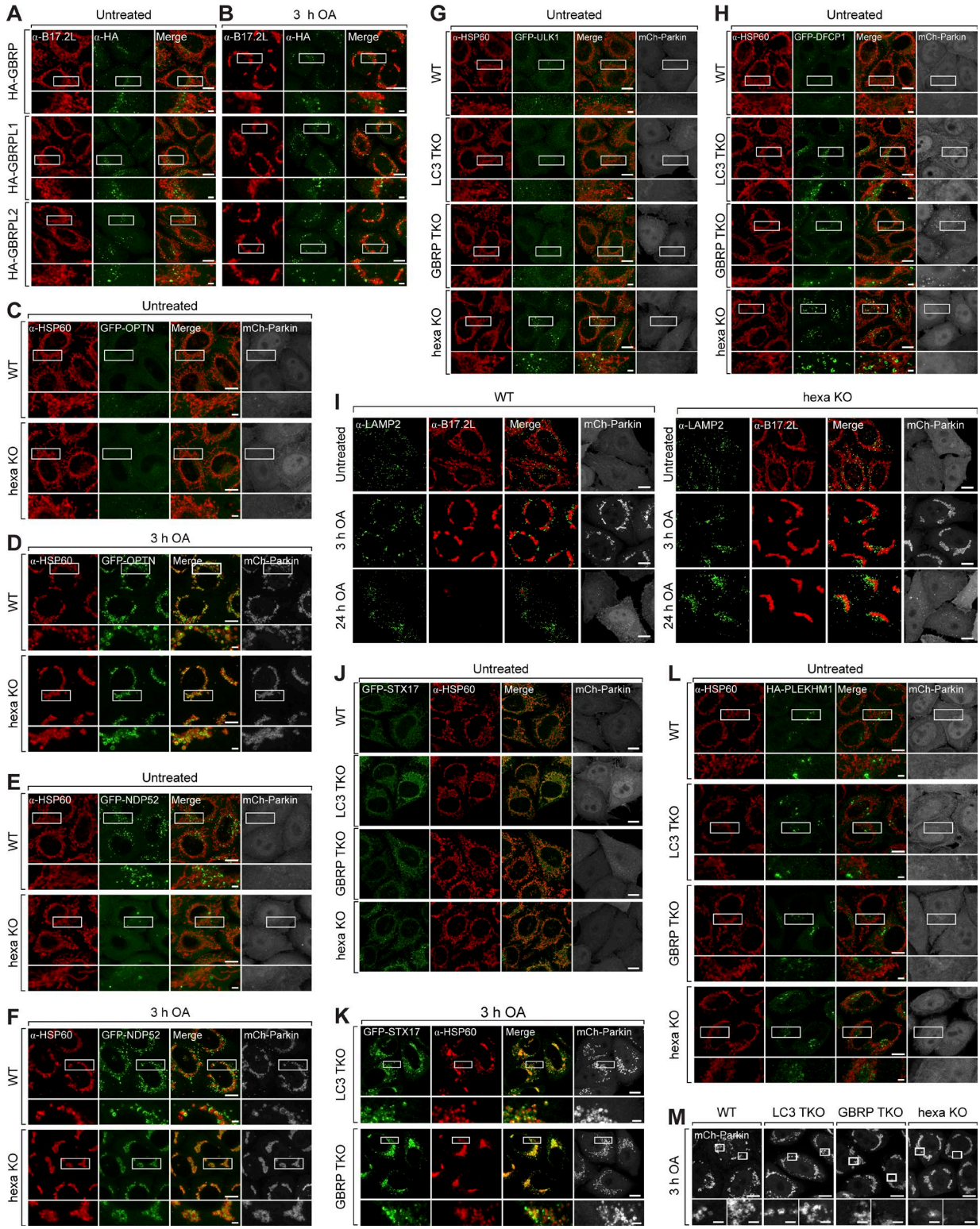

Figure S2. **Atg8s are dispensable for mitophagy receptor recruitment, formation of ULK1 foci and DFCP1 structures, lysosome translocation, and autophagosomal recruitment of STX17.** (A and B) Representative images of (A) untreated and (B) 3-h OA–treated hexa KO cells expressing untagged Parkin and HA-GBRP, HA-GBRPL1, or HA-GBRPL2, immunostained for B17.2L and HA. (C–F) Representative images of (C and E) untreated and (D and F) 3-h OA–treated WT and hexa KO cells expressing mCh-Parkin and either (C and D) GFP-OPTN or (E and F) GFP-NDP52, immunostained for HSP60 and GFP. (G and H) Representative images of untreated WT, LC3 TKO, GBRP TKO, and hexa KO cells, expressing either (G) GFP-ULK1 or (H) GFP-DFCP1, immunostained for HSP60 and GFP. (I) Representative images of untreated or OA-treated (times as indicated) WT and hexa KO cells expressing mCh-Parkin and immunostained for LAMP2 and B17.2L. (J and K) Representative images of untreated WT, LC3 TKO, GBRP TKO, and hexa KO cells (J) and 3-h OA–treated LC3 TKO, GBRP TKO cells (K) expressing mCh-Parkin and GFP-STX17, immunostained for HSP60 and GFP. (L) Representative images of untreated WT, LC3 TKO, GBRP TKO, and hexa KO cells expressing mCh-Parkin and HA-PLEKHM1, immunostained for HSP60 and HA. (M) mCh-Parkin channels corresponding to images presented in Fig. 9 E. Bars: 10 µm; (insets) 2 µm.

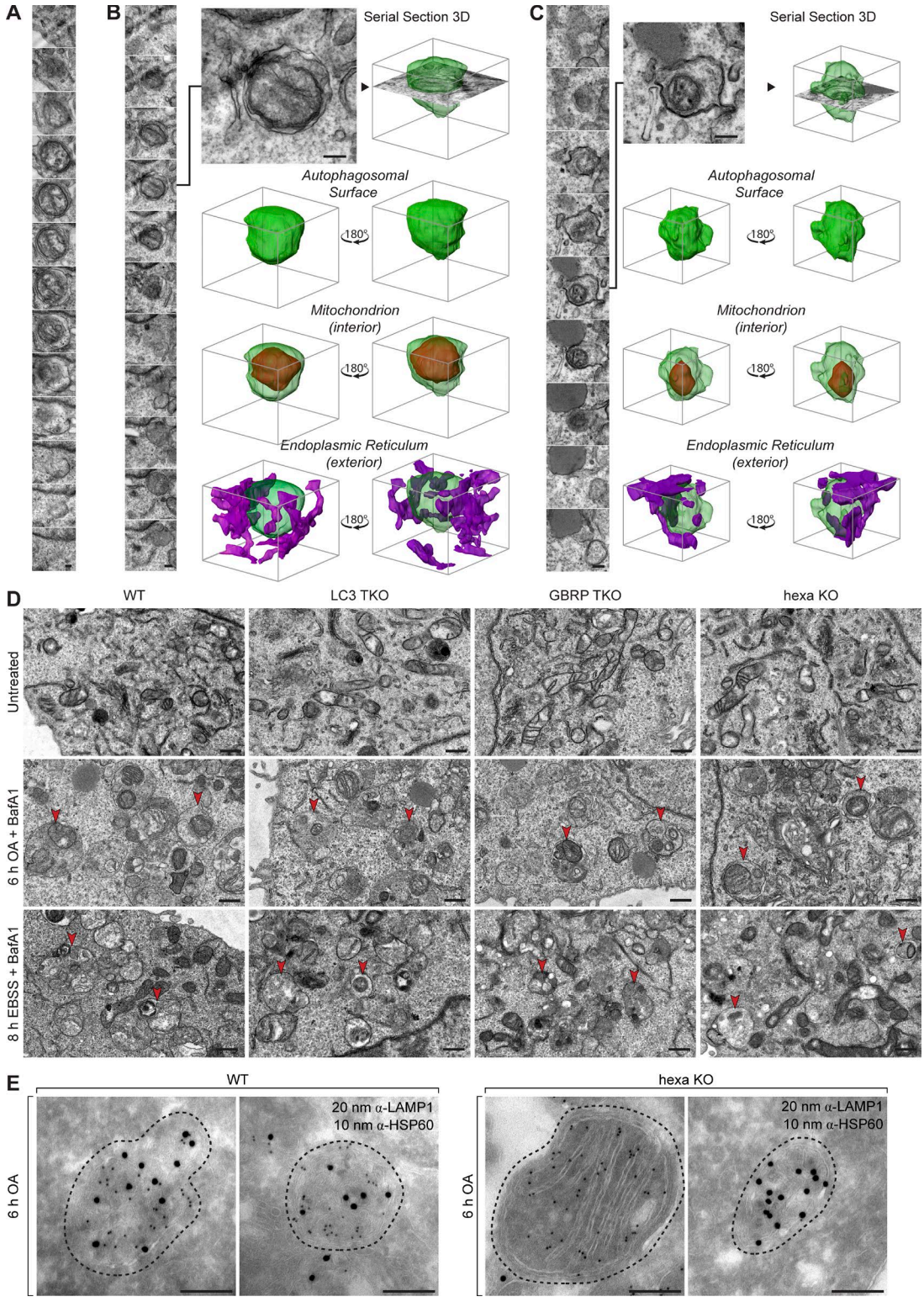

Figure S3. **Atg8s are dispensable for autophagosome biogenesis and closure during starvation and mitophagy.** (A) An image montage of serial sections used for 3D reconstruction of an autophagosome (see Fig. 3 E). (B and C) Additional 3D renderings of serial sectioned autophagosomal compartments (green) from hexa KO cells after 6-h OA and BafA1 treatment, displayed with sequestered mitochondrion (red) and endoplasmic reticulum (purple). (D) Representative TEM overview images of WT, LC3 TKO, GBRP TKO, and hexa KO cells without treatment, 6-h OA and BafA1 treatment, or 8-h starvation in EBSS and BafA1 (autophagosomes are indicated by arrowheads). (E) Representative immunogold TEM images of WT and hexa KO cells, dual labeled for LAMP1 (20 nm gold) and HSP60 (10 nm gold) after incubation with OA alone for 6 h (compartment perimeters indicated by offset dashed line). Bars: (A–C and E) 200 nm; (D) 500 nm.

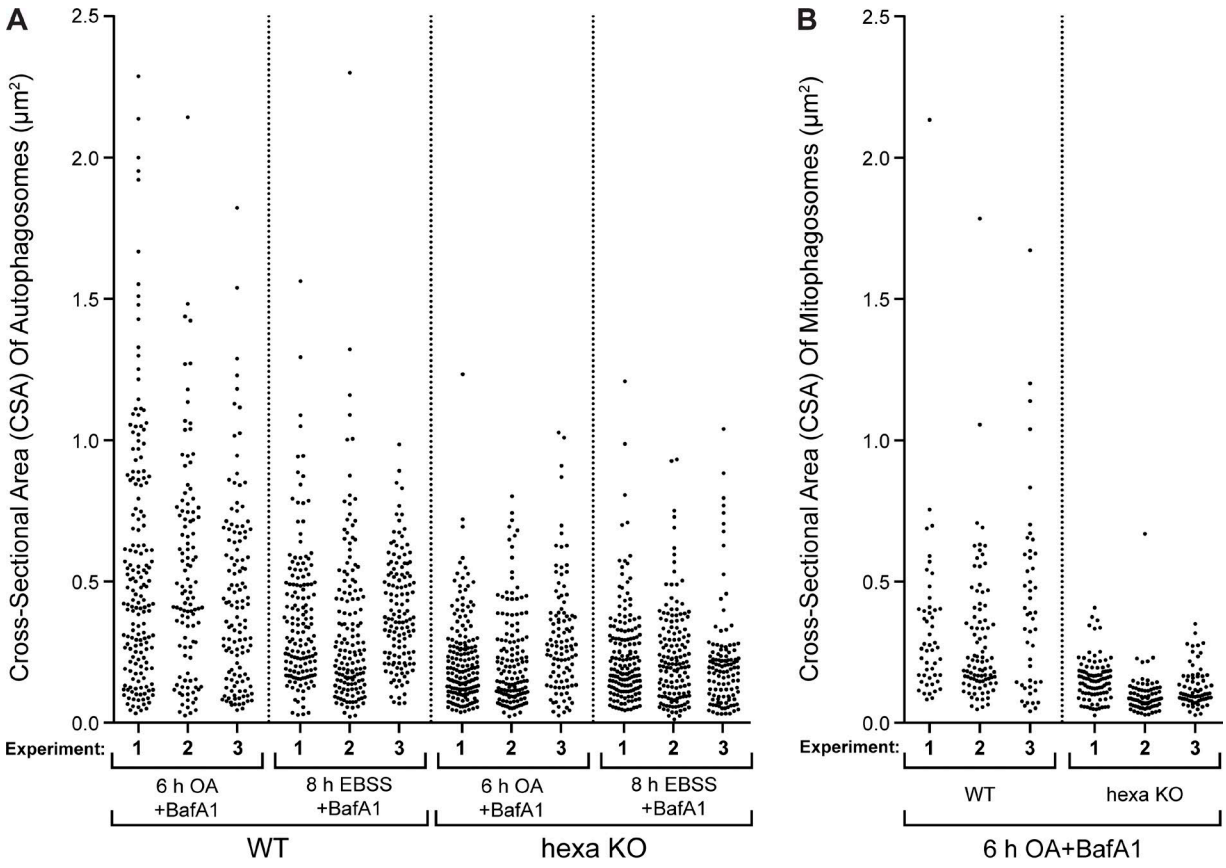

C

Mean Autophagosome Cross-Sectional Area (CSA)

	WT	hexa KO
Mitophagy	0.514 ± 0.034 μm²	0.253 ± 0.026 μm²
Starvation	0.369 ± 0.016 μm²	0.234 ± 0.009 μm²

Spherical autophagosome model

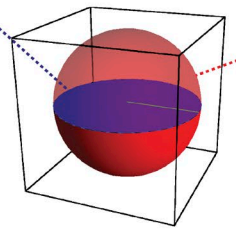

$V_{Sphere} = \frac{4}{3}\pi r^3$

$A_{Circle} = \pi r^2$

$\therefore V_{Sphere} = \frac{4\sqrt{CSA^3}}{3\sqrt{\pi}}$

hexa KO autophagosome volume relative to WT (%)

Autophagosome Volume (modeled)

	WT	hexa KO	Mean ± SEM	95% CI
Mitophagy	0.277 ± 0.028 μm³	0.096 ± 0.015 μm³	34.56 ± 0.71%	32.17% - 36.96%
Starvation	0.169 ± 0.012 μm³	0.085 ± 0.005 μm³	50.63 ± 0.15%	50.11% - 51.15%

Figure S4. **Atg8s regulate autophagosome size.** (A and B) Univariate scatter diagrams of the cross-sectional area measurements of (A) autophagosomes in WT and hexa KO cells after 6-h OA treatment with BafA1 or 8-h starvation in EBSS with BafA1 (see Fig. 3) and (B) mitophagosomes in WT and hexa KO cells after 6-h OA treatment with BafA1 (see Fig. 5). (G) The mean volumes of autophagosomes formed during mitophagy and starvation in WT and hexa KO cells were compared using Cavalieri's principle, a spherical autophagosome model, and TEM measurements of the cross-sectional area for autophagosomes under the conditions described in Fig. 3. Values in C are mean ± SEM.

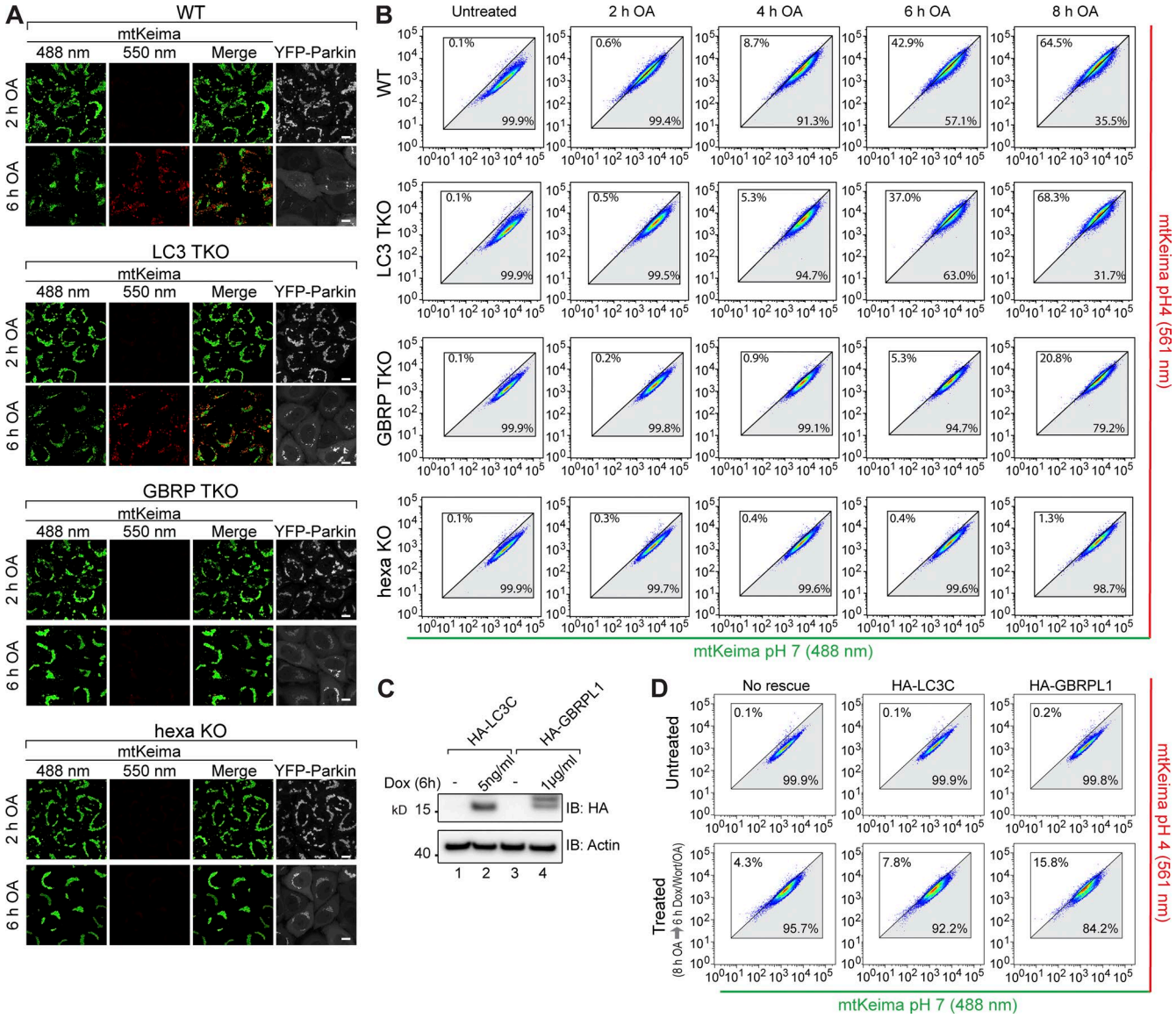

Figure S5. **GBRP TKO and hexa KO display a significant defect in autophagosome–lysosome fusion, which is rescued by introduction of GBRPL1, but not LC3C.** (A and B) WT, LC3 TKO, GBRP TKO, and hexa KO cells expressing YFP-Parkin and mtKeima untreated and treated with OA for the indicated times were analyzed by (A) fluorescence microscope and (B) FACS for lysosomal-positive mtKeima. (C) Immunoblotting to confirm the expression of HA-LC3C and HA-GBRPL1 upon Dox induction in Fig. 7 (C and D). (D) Hexa KO cells expressing mtKeima and Dox-inducible HA-LC3C or HA-GBRPL1 were pretreated with OA for 8 h. After being incubated with Dox, Wort, and OA for 6 h, the cells were analyzed by FACS for lysosomal-positive mtKeima. Bars, 10 μm.

Table S1. **Genotyping primers used for sequencing analysis of the knockout lines**

Gene	Exon	Primer direction	Primer sequence (5′ to 3′)	PCR product (bp)
MAP1LC3A	3	Forward	TCCTGGACAAGACCAAGTTTTT	460
		Reverse	GTGAAAGGCTGGGAATCATTCT	
MAP1LC3B	2	Forward	TGGCCCTTAGTAATGCTTCTGT	277
		Reverse	TAGGTTGTGAAACTGACACCCA	
MAP1LC3C	3	Forward	GTAAGACACCACTGGACTTCCG	349
		Reverse	CCAAAATAAAACTGCCAAACGA	
GABARAP	1	Forward	GTAGCAACACGGTTCGTGAATA	916
		Reverse	AATCAGACGGAGGTGACTTGTT	
GABARAPL1	2	Forward	GCAGCTATAACCTCATGAAGCC	763
		Reverse	GCTGTGTCAAAATCCAACAAGA	
GABARAPL2	2	Forward	ATGAAGTGGATGTTCAAGGAGG	912
		Reverse	AAAATATGGCAGAAGGGGTTTT	
STX17	4	Forward	TAAAGAAGAAGCATCAGCAGCA	270
		Reverse	CAAGGATTCAGCATATTGGGAT	
VPS39	1	Forward	GGTCTACCCTTAGCCCAGACTC	296
		Reverse	ATCCTAAGCCCCTCTCGTGTA	

Table S2. **Antibodies used in this study**

Antibodies	Company	Species	Catalog number (antigen used to make the antibody)
COXII	Abcam	Mouse	ab110258
GABARAPL1	Abcam	Rabbit	ab86497 (aa 1–50 of hGABARAPL1)
GABARAPL2	Abcam	Rabbit	ab126607 (synthetic peptide in hGABARAPL2)
HSP60	Abcam	Mouse	ab128567
LAMP2	Abcam	Mouse	ab25631
PLEKHM1	Abcam	Rabbit	ab204437
p62	Abnova	Mouse	H00008878-M01
Actin	Cell Signaling Technology	Rabbit	4967S
GABARAP	Cell Signaling Technology	Rabbit	13733S (residues surrounding Arg40 of hGABARAP)
HA	Cell Signaling Technology	Rabbit	3724S
LAMP1	Cell Signaling Technology	Rabbit	9091P
LC3A	Cell Signaling Technology	Rabbit	4599S (synthetic peptide near N terminus of hLC3A)
LC3B	Cell Signaling Technology	Rabbit	4108S (residues surrounding Gly40)
LC3C	Cell Signaling Technology	Rabbit	14736S (synthetic peptide near N terminus of hLC3C)
NDP52	Cell Signaling Technology	Rabbit	9036S
DNA	Progen Biotechnik	Mouse	61014
Parkin	Santa Cruz Biotechnology, Inc.	Mouse	sc-32282
TOM20	Santa Cruz Biotechnology, Inc.	Rabbit	sc-11415
TOM20	Santa Cruz Biotechnology, Inc.	Mouse	sc-17764
FLAG (M2)	Sigma-Aldrich	Mouse	F1804
STX17	Sigma-Aldrich	Rabbit	HPA001204 (aa 12–155)
OPTN	Proteintech	Rabbit	10837-1-AP

Table S3 is provided online as a PDF and shows details of CRISPR sequences, genotyping results of all knockout cell lines in this study.